

Naval Research Laboratory

Washington, DC 20375-5000



NRL Report 9345

Performance of an Angle-of-Arrival Estimator in the Presence of a Mainbeam Interference Source

FENG-LING C. LIN AND F. F. KRETSCHMER, JR.

*Target Characteristics Branch
Radar Division*

August 12, 1991

Approved for public release; distribution unlimited.



REPORT DOCUMENTATION PAGE

Form Approved
OMB No. 0704-0188

Public reporting burden for this collection of information is estimated to average 1 hour per response, including the time for reviewing instructions, searching existing data sources, gathering and maintaining the data needed, and completing and reviewing the collection of information, including suggestions for reducing this burden. Send comments to Washington Headquarters Service, Paperwork Project (0704-0188), 1215 Jefferson Davis Highway, Suite 1204, Arlington, VA 22202-4302, and to the Office of Management and Budget, Paperwork Project (0704-0188), 1215 Jefferson Davis Highway, Suite 1204, Arlington, VA 22202-4302.

1. AGENCY USE ONLY (Leave blank)		2. REPORT DATE August 12, 1991	3. REPORT TYPE AND DATES COVERED	
4. TITLE AND SUBTITLE Performance of an Angle-of-Arrival Estimator in the Presence of a Mainbeam Interference Source			5. FUNDING NUMBERS PE - 63319N TA - R1973 WU - DN156-470	
6. AUTHOR(S) Feng-Ling C. Lin and Frank F. Kretschmer, Jr.				
7. PERFORMING ORGANIZATION NAME(S) AND ADDRESS(ES) Naval Research Laboratory Washington, DC 20375-5000			8. PERFORMING ORGANIZATION REPORT NUMBER NRL Report 9345	
9. SPONSORING/MONITORING AGENCY NAME(S) AND ADDRESS(ES) Naval Sea Systems Command Washington, DC 20362-5101			10. SPONSORING/MONITORING AGENCY REPORT NUMBER	
11. SUPPLEMENTARY NOTES				
12a. DISTRIBUTION/AVAILABILITY STATEMENT Approved for public release; distribution unlimited.			12b. DISTRIBUTION CODE	
13. ABSTRACT (Maximum 200 words) Mainbeam interference presents a serious target tracking problem for array antennas. In this report we investigate a technique that is capable of providing information on target angle of arrival when a single interference source enters the antenna mainbeam. In-depth evaluation of the technique shows that its performance in angle estimation accuracy is comparable with that obtained by other more sophisticated methods, yet its implementation is relatively simple. The resultant angular estimation errors are quite close to the theoretical Cramer-Rao bounds previously derived.				
14. SUBJECT TERMS Angle estimation Mainbeam interference Squinted beams Adaptive arrays Cramer-Rao bound			15. NUMBER OF PAGES 17	
			16. PRICE CODE	
17. SECURITY CLASSIFICATION OF REPORT UNCLASSIFIED	18. SECURITY CLASSIFICATION OF THIS PAGE UNCLASSIFIED	19. SECURITY CLASSIFICATION OF ABSTRACT UNCLASSIFIED	20. LIMITATION OF ABSTRACT SAR	



CONTENTS

1. INTRODUCTION	1
2. SQUINTED-BEAM TECHNIQUE	2
3. ANGULAR ESTIMATION ERROR BASED ON SIMULATION	3
4. DEGRADATION OF TARGET RESPONSE BECAUSE OF INTERFERENCE	9
5. EFFECTS OF MAINBEAM NOT POINTING AT THE BORESIGHT	11
6. CONCLUSIONS	13
7. REFERENCES	13

PERFORMANCE OF AN ANGLE-OF-ARRIVAL ESTIMATOR IN THE PRESENCE OF A MAINBEAM INTERFERENCE SOURCE

1. INTRODUCTION

When an external interference source signal enters the antenna mainbeam region, it can mask the desired target echoes and impose severe limits on target detectability and accuracy of angle-of-arrival measurements. The objective of the study performed here is to investigate a technique capable of estimating target angle of arrival accurately by using both the sum and difference beams of a monopulse radar in which a single mainbeam interference source has been suppressed.

The target tracking problem in the presence of mainbeam interference was addressed in the literature by Davis, et al [1]. Based on the maximum likelihood theory, they proposed a relatively complicated angle-of-arrival estimator involving adaptively distorted sum and difference beams analogous to those used in a conventional monopulse antenna. Their simulation results have shown good performance for the cases of sidelobe and mainlobe interference.

Gabriel's approach, in Ref. 2, was to determine the monopulse error curve from the adapted sum and difference beams in which the interference signals have been suppressed. The resultant distorted error curve across the tracking angle region in the mainbeam was directly used to determine the angle of arrival of the target. This approach was further analyzed by Lin and Kretschmer [3,4]. In Refs. 3 and 4, Monte Carlo simulations were performed, and the Cramer-Rao (C-R) bounds on the angular estimation error were obtained. Simulation results demonstrated that very good performance on angular estimation accuracy could be achieved as compared with the theoretical lower bounds.

Gabriel's approach requires a fully adaptive implementation, estimating the covariance matrix of interference plus noise, and calculating the covariance matrix inverse. These can be easily done for a small array antenna. In practice, the covariance matrix must be estimated from a finite number of range cells (snapshots). It was found in Refs. 3 and 4 that the simulated angle errors are closer to the C-R bounds for larger target-interference angular separations. As the angular separation decreases, more snapshots are required for the simulated angle errors to approach the bounds. For larger arrays, it becomes increasingly difficult to accurately estimate the covariance matrix and calculate its inverse. Instead of forming the adapted sum and difference beams through the "element space" as employed in Gabriel's approach, a simplified technique through the "beam space" capable of providing comparably good angle estimates is highly desirable.

In this report, a squinted-beam technique is described. In-depth evaluation of the technique is performed to determine the feasibility of the technique in achieving good angle of arrival estimation when a single interference source is present in the antenna mainbeam. The resultant angular estimation errors are then compared with the C-R bounds derived in earlier reports [3,4].

2. SQUINTED-BEAM TECHNIQUE

A linear-array antenna of N equally spaced elements is used in the squinted-beam technique, and Fig. 1 shows the array geometry. In this report, we describe the one-dimensional (1-D) problem of obtaining the target azimuthal angle of arrival, which is generally of most interest. However, the technique can be extended to elevation angle estimation above the region where multipath is a problem. We assume that N is even ($N = 2M$), and the phase center of the array coincides with the center of the array. With the two halves of the array, represented by A and B , fed in phase (the sum mode, $\Sigma = A + B$), one obtains a pattern with a single mainbeam. When the two halves of the aperture are excited out of phase (the difference mode, $\Delta = A - B$), a pattern with a null between the two principal lobes is formed.

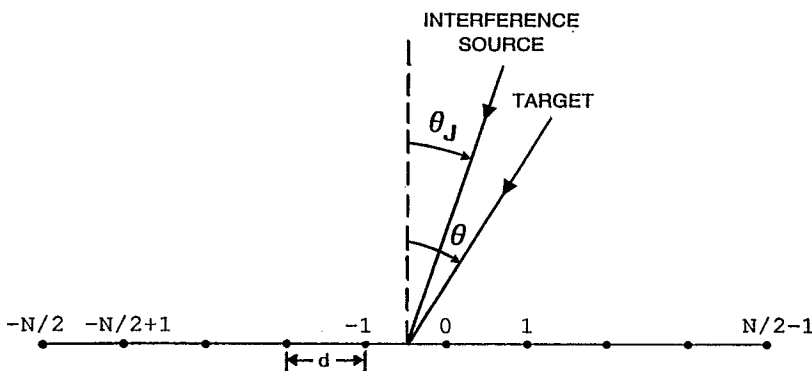


Fig. 1 — Array geometry

Assume that the angle of arrival of the external interference source θ_J has been determined. The radar sum pattern is then steered toward the known interference source direction, which is also in the null of the difference pattern. Subsequently, as Fig. 2 shows, two squinted beams, C and D , are formed with a differential squint angle of $-\alpha$ and α , respectively, relative to the mainbeam direction. In this technique, the difference beam is not used for angle estimation as in the case of regular monopulse tracking but is used for target detection, which will be described in Section 4.

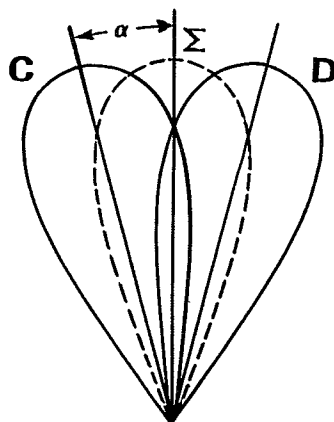


Fig. 2 — Squinted beams

With the antenna mainbeam pointing in the direction of the interference source, two adaptive cancelers are used with C and D as auxiliary inputs and Σ as the main input (Fig. 3). The optimum weights W_C and W_D achieved by the two open-loop cancelers are determined in a target-free region such that the interference in the mainbeam is canceled in the interference source direction. We assume that the responses of Σ , C , and D to the interference at θ_J are Σ_J , C_J , and D_J , respectively. As in Ref. 5, these optimum weights are given by [5]

$$W_C = \frac{\overline{\Sigma_J C_J^*}}{\overline{C_J C_J^*}}$$

and (1)

$$W_D = \frac{\overline{\Sigma_J D_J^*}}{\overline{D_J D_J^*}}.$$

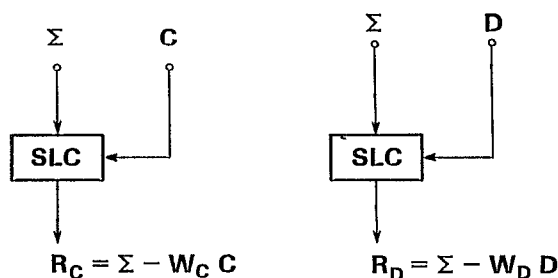


Fig. 3 — Canceler configurations

When a target is present in the antenna mainbeam at θ , the residues R_C and R_D of the target signal out of the two cancelers can be expressed as

$$R_C = \Sigma_T - W_C C_T$$

and (2)

$$R_D = \Sigma_T - W_D D_T$$

where Σ_T , C_T , and D_T are the target responses of Σ , C , and D at θ (Fig. 4). In general, R_C and R_D , as a function of θ , have different magnitudes and signs. If the ratio $|R_C/R_D|$ were a monotonic function of θ_T , the angular separation between the target and the interference source ($\theta_T = \theta - \theta_J$), the ratio would provide a calibration error curve for determining the target angle of arrival relative to the interference source direction.

We first assume that the interference source direction is at the antenna boresight ($\theta_J = 0^\circ$). The effects of steering the Σ beam off boresight are described in Section 5. For an array of N -elements, the two halves of the array pattern, A and B , can be written as

$$A = \sum_{i=-M}^{-1} a_i e^{j \left(\frac{2\pi}{\lambda} \right) \left(i + \frac{1}{2} \right) d \sin \theta}$$

and (3)

$$B = \sum_{i=0}^{M-1} a_i e^{j \left(\frac{2\pi}{\lambda} \right) \left(i + \frac{1}{2} \right) d \sin \theta},$$

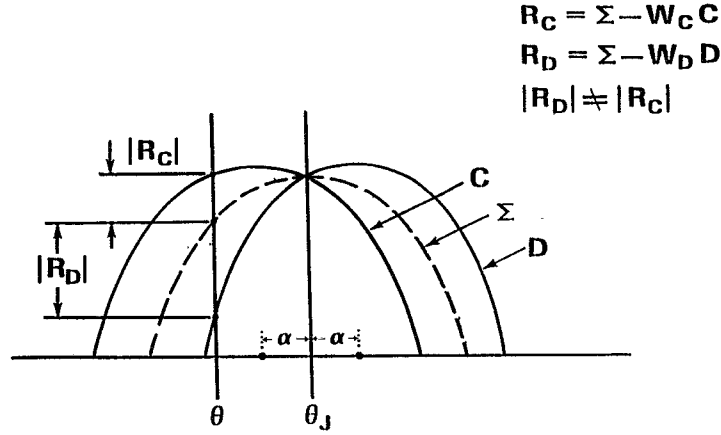


Fig. 4 — Differentially squinted antenna patterns

where

$$M = N/2,$$

a_i is the weighting function applied to the array elements,

d is the spacing between array elements,

λ is the radar wavelength, and

θ is the target angle of arrival ($\theta = \theta_{TJ}$, when $\theta_J = 0^\circ$).

The sum beam is then given by

$$\Sigma = \sum_{i=-M}^{M-1} a_i e^{j \left(\frac{2\pi}{\lambda} \right) \left(i + \frac{1}{2} \right) d \sin \theta} \quad (4)$$

The two squinted beams, C and D , are formed when the sum pattern is steered to an angle $-\alpha$ and α by applying linearly progressive phase increments from element to element, so that the phase between adjacent elements differs by $-(2\pi d/\lambda) \sin \alpha$ and $(2\pi d/\lambda) \sin \alpha$, respectively. The two squinted beams, C and D , are expressed by

$$C = \sum_{i=-M}^{M-1} a_i e^{j \left(\frac{2\pi}{\lambda} \right) \left(i + \frac{1}{2} \right) d (\sin \theta + \sin \alpha)} \quad (5)$$

and

$$D = \sum_{i=-M}^{M-1} a_i e^{j \left(\frac{2\pi}{\lambda} \right) \left(i + \frac{1}{2} \right) d (\sin \theta - \sin \alpha)}$$

To cancel the interference in the sum beam along the interference source direction, the optimum canceler weights in Eq. (1) reduce to

$$W_C = \frac{\Sigma_o}{C_o}$$

and

$$W_D = \frac{\Sigma_o}{D_o}, \quad (6)$$

where

$$\Sigma_0 = \sum_{i=-M}^{M-1} a_i,$$

$$C_0 = \sum_{i=-M}^{M-1} a_i e^{j\left(\frac{2\pi}{\lambda}\right)\left(i+\frac{1}{2}\right) d \sin\alpha},$$

and

(7)

$$D_0 = \sum_{i=-M}^{M-1} a_i e^{-j\left(\frac{2\pi}{\lambda}\right)\left(i+\frac{1}{2}\right) d \sin\alpha}$$

are the responses of the sum and the two squinted beams, C and D , in the direction of interference, which is also the antenna boresight. The canceler residues R_C and R_D are calculated from Eq. (2). The calibrated error curves are obtained by taking the absolute value of the ratio R_C/R_D as a function of θ . Figure 5 shows these calibration error curves in the mainbeam region for squint angles from 0.1 to 1.0 θ_{BW} with a cosine weighting applied to an 8-element antenna array. Here θ_{BW} is the 3 dB beamwidth of the sum beam in Eq. (4). Note that the ratio $|R_C/R_D|$, undefined in the interference source direction, is assumed to be one. Throughout the study, the array elements are assumed to have a spacing of $\lambda/2$. Similarly, Fig. 6 illustrates the calibration curves with a Hamming weighting instead of a cosine weighting. It is shown that the slopes of these curves are different from unity and are very much dependent on the squint angle and the element weighting. These calibration curves are used in determining the target angle of arrival based on the ratio $|R_C/R_D|$ obtained from the actual measurements.

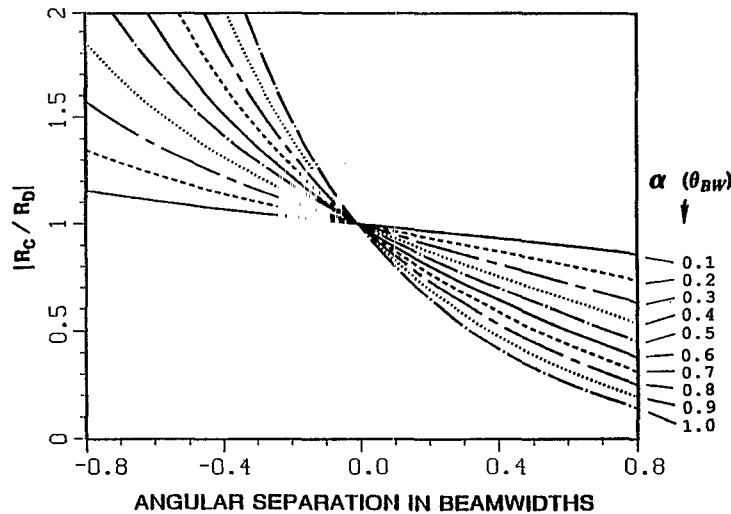


Fig. 5 — $|R_C/R_D|$ as a function of angular separation for squint angles of $\alpha = 0.1 - 1.0 \theta_{BW}$; $N = 8$, $\theta_j = 0$ and cosine weighting

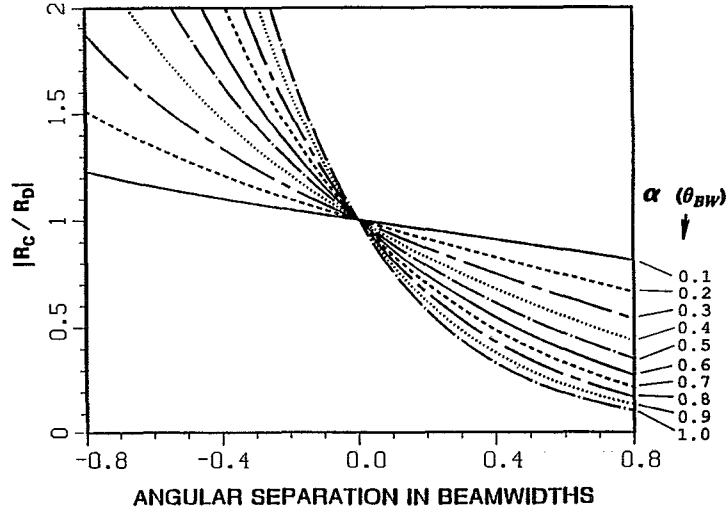


Fig. 6 — $|R_C/R_D|$ as a function of angular separation for squint angles of $\alpha = 0.1 - 1.0 \theta_{BW}$; $N = 8$, $\theta_J = 0$ and Hamming weighting

3. ANGULAR ESTIMATION ERROR BASED ON SIMULATION

To estimate the errors in determining the angle of arrival in the presence of mainbeam interference, Monte Carlo simulation is performed based on the estimation procedure described in Section 2. The received complex target plus interference signal X_k at the k th element of an N -element weighted array is given by

$$X_k = a_k \left[s e^{j \left(\frac{2\pi}{\lambda} \right) \left(k + \frac{1}{2} \right) d \sin \theta} + r_J e^{j \left(\frac{2\pi}{\lambda} \right) \left(k + \frac{1}{2} \right) d \sin \theta_J} + n_k \right], \quad (8)$$

where

- a_k is the weighting function,
- s is the complex target echo received at the center of the array,
- θ is the angle of arrival of the target,
- r_J is the received signal of the interference source at the center of the array,
- θ_J is the angle of arrival of the interference source,
- n_k is the thermal noise at the k th element, and
- $k = -M, -M + 1, \dots, M - 1$.

The signal is assumed to be processed in time-sampled, digitized inphase and quadrature channels. The received squinted beam returns C_k and D_k at the k th element of the N -element array are

$$C_k = a_k \left[s e^{j \left(\frac{2\pi}{\lambda} \right) \left(k + \frac{1}{2} \right) d (\sin \theta + \sin \alpha)} + r_J e^{j \left(\frac{2\pi}{\lambda} \right) \left(k + \frac{1}{2} \right) d \sin \alpha} + n_k \right] \quad (9)$$

and

$$D_k = a_k \left[s e^{j \left(\frac{2\pi}{\lambda} \right) \left(k + \frac{1}{2} \right) d (\sin \theta - \sin \alpha)} + r_J e^{-j \left(\frac{2\pi}{\lambda} \right) \left(k + \frac{1}{2} \right) d \sin \alpha} + n_k \right].$$

Here the interference source is assumed at the antenna boresight; i.e., $\theta_J = 0^\circ$ or $\theta = \theta_{TJ}$. We will estimate and compute the error of θ_{TJ} , the angle of arrival of the desired signal measured from the interference source direction, in the presence of internal noise and an external interference source.

Random complex Gaussian variables are generated to represent an interference source and receiver noise. The received signals X_k , C_k , and D_k , as defined in Eqs. (8) and (9), are determined, and each

realization of these values is referred to as a run. Let I be the noise power of the interference source and N_o be the thermal noise power that is assumed to be the same for each element. By using the weights W_C and W_D obtained previously (Eq. (6)) in determining the calibration curves for the interference-only case, the ratio

$$\left| \frac{R_C}{R_D} \right| = \left| \frac{\sum_{k=M}^{M-1} (X_k - W_C C_k)}{\sum_{k=M}^{M-1} (X_k - W_D D_k)} \right| \tag{10}$$

is obtained for each run. Then K independent samples of this ratio are averaged before the angle θ_{TJ} is estimated by using the calibration curves obtained previously. The results presented here are based on repeating the above process of angle estimation 100 times.

In the simulation the following conditions are assumed. An 8-element linear antenna array is used to receive the signal consisting of returned echoes from a target with a signal-to-noise ratio per element S/N_o of 10 dB and from an interference source with $I/N_o = 30$ dB per element. The array elements are cosine weighted. With the radar sum beam pointed toward the interference source, two squinted beams, C and D , are generated with differential squint angles of $-\alpha$ and α , respectively, from the mainbeam peak. The target-interference source angular separation is varied from $0.1 \theta_{BW}$ to $1.0 \theta_{BW}$ with a step size of $0.1 \theta_{BW}$. The simulated results of σ_μ , the rms $\sin \theta_{TJ}$ estimate error normalized to $\sin \theta_{BW}$, are obtained. Note that σ_μ is very close to the angular estimation error in beamwidths [3,4]. Figures 7 and 8 show the results in dashed lines for the case $\alpha = 0.3 \theta_{BW}$ with four different values of K ($K = 1, 8, 16,$ and 32). The solid lines are the theoretical C-R bounds on the angular estimation errors that have been derived in Refs. 3 and 4. The individual data points are the results obtained from Gabriel's approach [3,4]. It is shown through simulation that the angular estimation error by using the squinted-beam technique is quite close to that obtained by using Gabriel's approach and is not far from the C-R bound. When the target-interference angular separation is near $0.2 \theta_{BW}$, the error is very close to $0.1 \theta_{BW}$ for $K = 8$ and decreases as K increases. For increasing angular separations the errors are within $0.1 \theta_{BW}$ for $K \geq 8$. It is also found that the errors are identical when the target is at either side of the interference source when the angular separation from the source is equal.

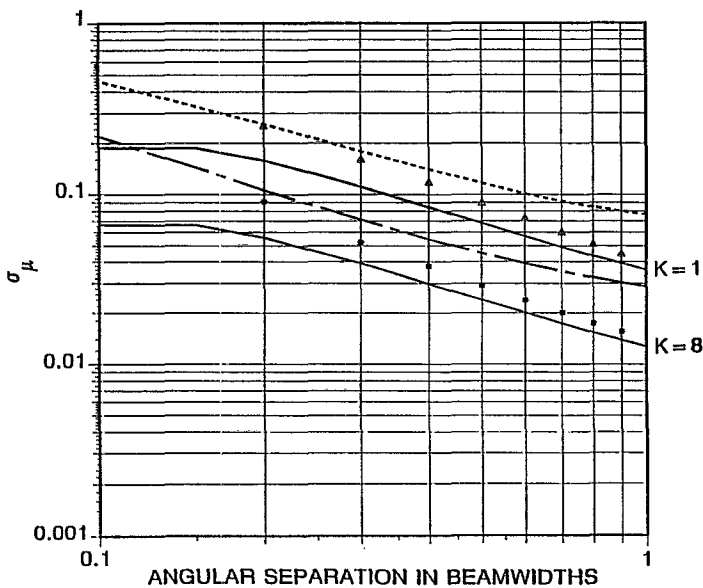


Fig. 7 — The Cramer-Rao bound (—), data from Gabriel's approach: $K = 1$ ($\Delta \Delta \Delta$) and $K = 8$ ($\blacksquare \blacksquare \blacksquare$), and the squinted-beam technique: $K = 1$ (---) and $K = 8$ (—), of σ_μ as a function of angular separation: $N = 8$, $S/N_o = 10$ dB, $I/N_o = 30$ dB, $\theta_j = 0$, and $\alpha = 0.3 \theta_{BW}$

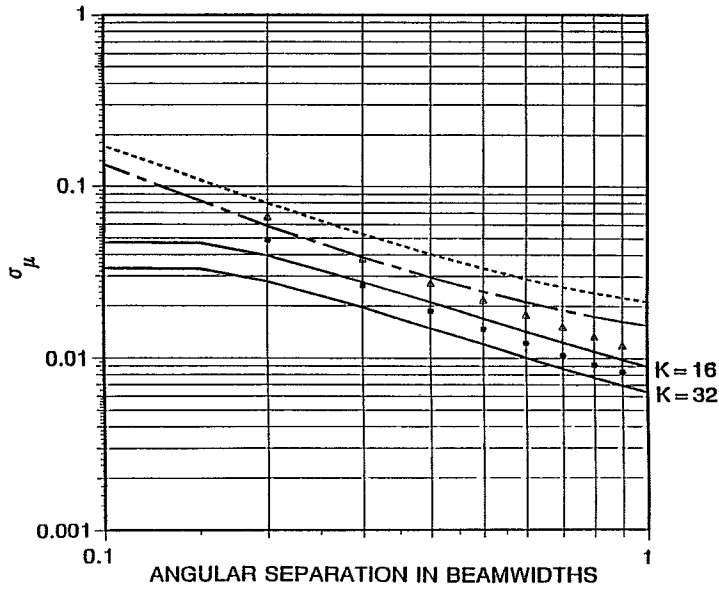


Fig. 8 — The Cramer-Rao bound (—), data from Gabriel's approach: $K = 16$ ($\Delta\Delta\Delta$) and $K = 32$ ($\blacksquare\blacksquare\blacksquare$), and the squinted-beam technique: $K = 16$ (---) and $K = 32$ (—), of σ_μ as a function of angular separation: $N = 8$, $S/N_o = 10$ dB, $I/N_o = 30$ dB, $\theta_j = 0$, and $\alpha = 0.3 \theta_{BW}$

Since the slope of $|R_C/R_D|$ is a function of the squint angle, simulations are also performed for various squint angles ranging from $0.05 \theta_{BW}$ to $1.0 \theta_{BW}$. Figure 9 shows the results under the same conditions described above when eight independent samples are averaged before estimating the angle of arrival. The estimated angle error is shown to be near the minimum when the squint angle α is between $0.1 \theta_{BW}$ and $0.075 \theta_{BW}$. The angular estimation error increases drastically from the minimum when α is decreased to $0.05 \theta_{BW}$.

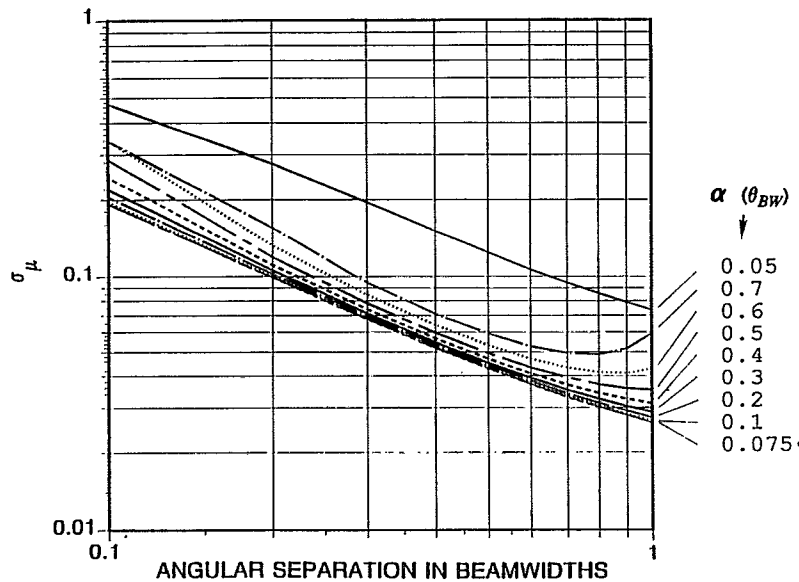


Fig. 9 — Simulated data of σ_μ as a function of angular separation for different squint angles: $N = 8$, $S/N_o = 10$ dB, $I/N_o = 30$ dB, $\theta_j = 0$, and $K = 8$

4. DEGRADATION OF TARGET RESPONSE BECAUSE OF INTERFERENCE

Next, we consider the target response degradation after interference nulling. The adapted sum beam patterns R_C and R_D , distorted because of mainbeam nulling, are shown in Fig. 10 for an 8-element, cosine-weighted array with a squint angle of $0.5 \theta_{BW}$ as an example. It is evident in Fig. 10 that when the target is closer to the interference source, the target response gets smaller. A relevant measure of the target response degradation is the output target-to-internal noise pattern ratio T/N . In Fig. 11, the greater T/N of the two adapted sum beam patterns, R_C and R_D , normalized by the interference-free T/N , is plotted as a function of θ_{TJ} for various values of the squint angle. For the interference-free case, T/N is calculated by using the antenna sum beam, Σ_T , and the fact that the internal noise power is normalized to one. Figure 12 shows similar plots as those in Fig. 11 for an 8-element array with a Hamming weighting. The degradation in T/N response increases as the target-interference angular separation decreases. This degradation also depends on the squint angle of the two squinted beams and the element weighting employed.

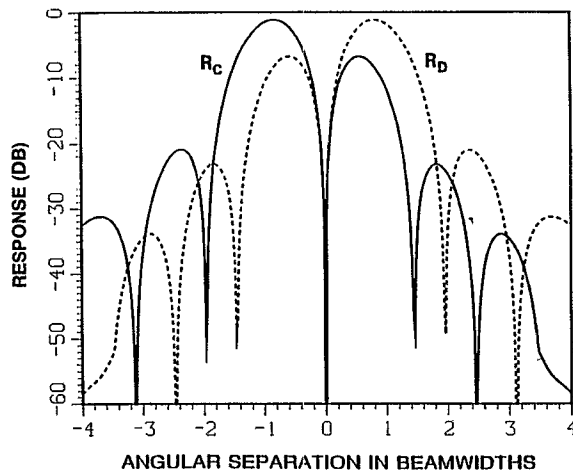


Fig. 10 — Adapted sum beam patterns, R_C (—) and R_D (---): $N = 8$, $\alpha = 0.5 \theta_{BW}$, and cosine weighting

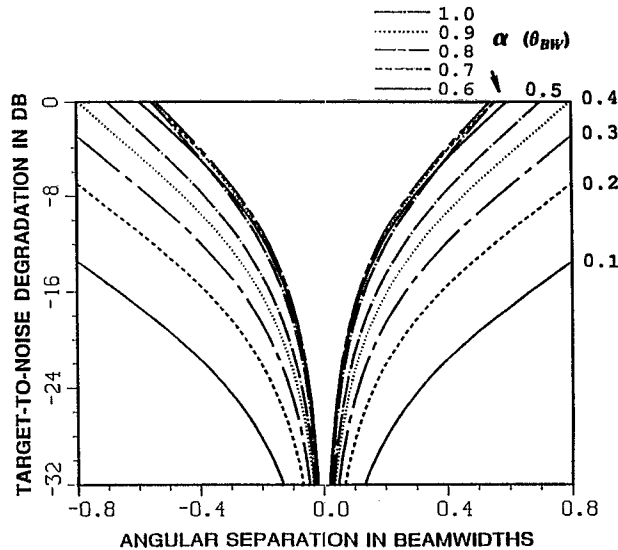


Fig. 11 — Target-to-noise ratio with respect to no interference case as a function of angular separation for squint angles of $\alpha = 0.1 - 1.0 \theta_{BW}$: $N = 8$, $\theta_j = 0$, and cosine weighting

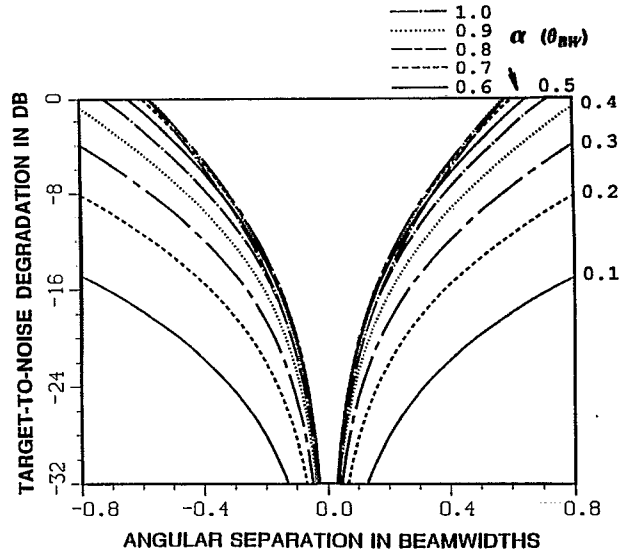


Fig. 12 — Target-to-noise ratio with respect to no interference case as a function of angular separation for squint angles of $\alpha = 0.1 - 1.0 \theta_{BW}$; $N = 8$, $\theta_j = 0$, and Hamming weighting

The adapted sum beam patterns could be used for target detection. For example, with $\alpha = 0.1 \theta_{BW}$, a target located at $0.3 \theta_{BW}$ from the interference source suffers a degradation of 24.5 dB in T/N as compared with the interference-free case (Fig. 11). This loss can be reduced to about 11 dB if $\alpha = 0.5 \theta_{BW}$ and be further reduced to about 7 dB if $\alpha = 0.8 \theta_{BW}$ (Fig. 11). However, the angular estimation error increases when α is increased from 0.1 to $0.8 \theta_{BW}$ (Fig. 9). One way to get around the T/N degradation problem is to use the difference beam Δ , where $\Delta = A - B$, for target detection. Figure 13 shows the difference pattern with one cycle of a sine weighting across the aperture of the 8-element array. When the target is at $0.3 \theta_{BW}$ from the interference source that is at the antenna boresight, the target degradation is about 4 dB. This is less than the case when the adapted sum beam pattern with a large squint angle (e.g., $\alpha = 0.8 \theta_{BW}$) is used for target detection.

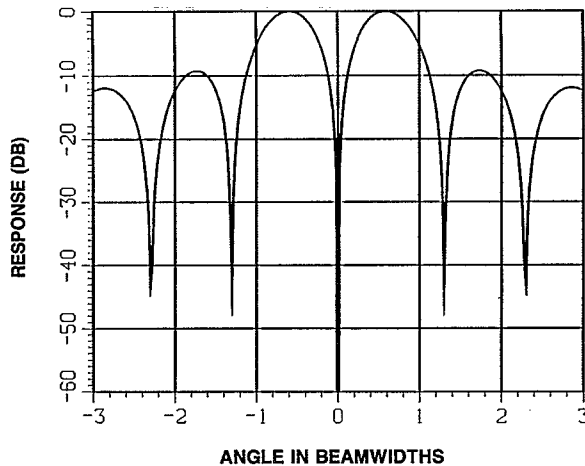


Fig. 13 — Difference pattern with sine weighting: $N = 8$

The sidelobe level of the sine-weighted difference pattern, however, is very high (about -9 dB). It is desirable to have a difference pattern with low sidelobes such as the Bayliss weighting. Figure 14 shows the Bayliss difference pattern with a -45 dB sidelobe level. The degradation in target response when $\theta_{TJ} = 0.3 \theta_{BW}$ is about 5 dB, which is slightly higher than the case with a sine weighting. However, within θ_{BW} the loss in target response is less than 5 dB if θ_{TJ} is greater than $0.3 \theta_{BW}$.

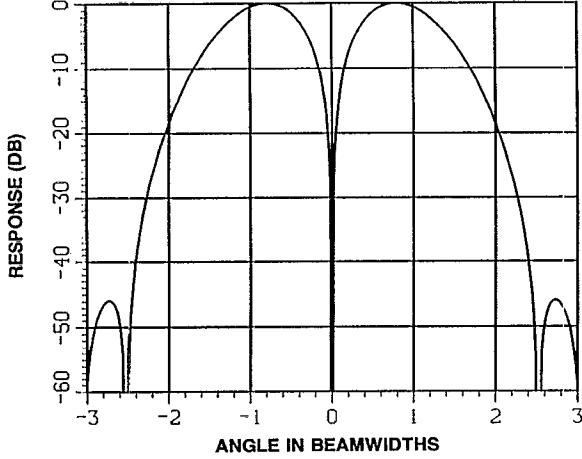


Fig. 14 — Bayliss difference pattern with sidelobe level of -45 dB; $N = 8$

5. EFFECTS OF MAINBEAM NOT POINTING AT THE BORESIGHT

So far we have only considered the case where the interference source is at the antenna boresight. When the mainbeam is pointed toward an interference source not at boresight, the shape of the mainbeam is distorted and becomes unsymmetrical with respect to the peak of the mainbeam:

$$\Sigma = \sum_{i=-M}^{M-1} a_i e^{j\left(\frac{2\pi}{\lambda}\right)\left(i+\frac{1}{2}\right) d (\sin\theta - \sin\theta_j)} \quad (11)$$

Also, the beam shapes of the two squinted beams, C and D , formed with differential squint angles of $-\alpha$ and α are not symmetrical with respect to the respective beam maximum:

$$C = \sum_{i=-M}^{M-1} a_i e^{j\left(\frac{2\pi}{\lambda}\right)\left(i-\frac{1}{2}\right) d (\sin\theta - \sin(\theta_j - \alpha))} \quad (12)$$

and

$$D = \sum_{i=-M}^{M-1} a_i e^{j\left(\frac{2\pi}{\lambda}\right)\left(i+\frac{1}{2}\right) d (\sin\theta - \sin(\theta_j + \alpha))}$$

The magnitudes of the patterns of the beams C and D in the interference direction, i.e., C and D evaluated at $\theta = \theta_j$, are then different. To cancel the interference in Σ , C and D are used as the auxiliary inputs to two adaptive cancelers whose main inputs are Σ (Fig. 3). The weights obtained in the interference source direction have different magnitudes ($|W_C| \neq |W_D|$). The resultant calibration curves, $|R_C/R_D|$ are also different from the cases where the interference source is at the boresight. For example, Fig. 15 shows the calibration curves for the case $\theta_j = 1.0 \theta_{BW}$ and cosine weighting on an 8-element array for squint angles $\alpha = 0.1 \theta_{BW}$ to $1.0 \theta_{BW}$. Note that the ratio $|R_C/R_D|$ undefined in the interference source direction is assumed to be one. Because of the asymmetry of the two squinted beams, the ratios $|R_C/R_D|$ are quite different from one near the interference source direction. This results in discontinuities or dips in the calibration curves in the vicinity of the interference source direction.

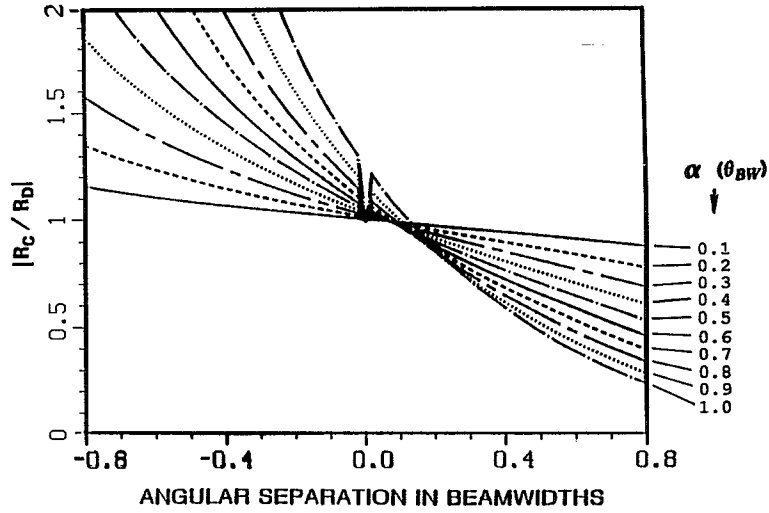


Fig. 15 — $|R_C/R_D|$ as a function of angular separation for squint angles of $\alpha = 0.1 - 1.0 \theta_{BW}$; $N = 8$, $\theta_j = 1.0 \theta_{BW}$, and cosine weighting

Figure 16 shows the simulation results of the angular estimation error for $K = 1$ when the mainbeam is steered toward different interference source directions and the target-interference angular separation is $\pm 0.4 \theta_{BW}$. For a fixed value of $|\theta_{TJ}|$, the error is less for a target near boresight than for a target near the endfire of the antenna. In addition, the error increases as the sum beam is steered away from the antenna boresight. Similar results are obtained for larger K values.

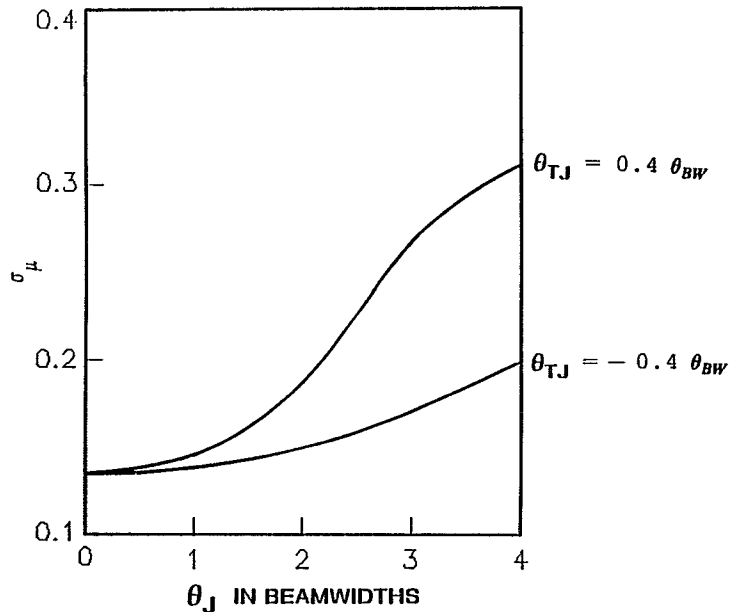


Fig. 16 — Simulated data of σ_μ as a function of interference source location for $\theta_{TJ} = 0.4 \theta_{BW}$; $N = 8$, $S/N_o = 10$ dB, $I/N_o = 30$ dB, $\alpha = 0.1 \theta_{BW}$, and $K = 1$

6. CONCLUSIONS

An investigation is performed on a squinted-beam technique that is capable of estimating the angle of arrival of a desired signal with a single mainbeam interference source suppressed. An adaptive array antenna is incorporated. Two squinted beams, C and D , with differential squint angles of $-\alpha$ and α are formed. The interferences in the squinted beams are used to cancel the interference in the mainbeam by two adaptive cancelers. The absolute values of the ratios of the residues from the two cancelers $|R_C/R_D|$ provide the necessary calibration curves across the entire mainbeam tracking region. A Monte Carlo simulation is performed on the estimation procedure described herein to evaluate the technique. The target angular estimation errors are obtained and then compared with the previously derived C-R bounds and also with the simulated results by using Gabriel's approach [3,4].

An 8-element equally spaced linear array having a cosine weighting, a target with $S/N_o = 10$ dB per element, and a single interference source with $I/N_o = 30$ dB per element are considered here. The technique is evaluated with a priori knowledge of θ_j for various squint angles and target-interference angular separations. It is first assumed that the interference source is at the antenna boresight. For all target-interference angular separations within the 3-dB beamwidth, the best angular estimation accuracy is achieved when α is very close to $0.1 \theta_{BW}$. At $\alpha = 0.1 \theta_{BW}$, the errors are within $0.1 \theta_{BW}$ as the target-interference angular separation is equal to or greater than $0.2 \theta_{BW}$, and at least eight independent samples of $|R_C/R_D|$ measurements are processed. Severe target-to-noise ratio degradation would be avoided if the adapted sum beams were not used for target detection. Instead, only a few dB loss in target-to-noise ratio result when a Bayliss difference pattern with very low sidelobes is adopted for detecting the target.

In the presence of a single interference source, the squinted-beam technique described here can be easily implemented, and the angular estimation procedure is simpler than the "element-space" technique, such as that used in Gabriel's approach. For the case where the interference source direction is at the antenna boresight, the performance of the squinted-beam technique described here is comparable with that obtained in Refs. 3 and 4 by using Gabriel's approach, and the angular estimation errors are quite close to the theoretical lower bounds. In Refs. 3 and 4, both the target and the interference source directions are constrained within the antenna mainbeam at boresight. When the interference source is not at the antenna boresight, the sum beam is then steered toward the interference source. In this case, for a given $|\theta_{TJ}|$ ($|\theta_{TJ}| < \theta_{BW}$) and $|\theta_J|$, the squinted-beam technique provides better target angle estimation if the target direction is closer to the antenna boresight than the interference source direction. Furthermore, with constant θ_{TJ} , target angular estimation accuracy degrades with increasing θ_j . In the presence of multiple interference sources, however, the squinted-beam technique cannot be applied, while Gabriel's approach may still be effective.

7. REFERENCES

1. R. C. Davis, L. E. Brennan, and L. S. Reed, "Angle Estimation with Adaptive Arrays in External Noise Fields," *IEEE Trans. Electron. Syst.* AES-12, 179-186 (1976).
2. W. F. Gabriel, "A High-Resolution Target-Tracking Concept Using Spectral Estimation Techniques," NRL Report 8797, May 1984.
3. F. C. Lin and F. Kretschmer, Jr., "Angle Estimation in the Presence of Mainbeam Interference," NRL Report 9234, Dec. 1989.
4. F. C. Lin and F. Kretschmer, Jr., "Angle Measurement in the Presence of Mainbeam Interference," *The Record of the IEEE 1990 International Radar Conference*, 444-450, May 1990.
5. F. F. Kretschmer, Jr. and B. L. Lewis, "A Digital Open-Loop Adaptive Processor," *IEEE Trans. Electron. Syst.* AES-14, 165-171 (1978).

